THE JOURNAL OF PHYSICAL CHEMISTRY B

ARTICLE

pubs.acs.org/JPCB

Role of Protein Dynamics in Guiding Electron-Transfer Pathways in Reaction Centers from *Rhodobacter sphaeroides*

Haiyu Wang,*[,†,‡] Yawei Hao,[†] Ying, Jiang,[†] Su Lin,[‡] and Neal W. Woodbury*[,‡]

[†]State Key Laboratory on Integrated Optoelectronics, College of Electronic Science and Engineering, Jilin University, 2699 Qianjin Street, Changchun 130012, China

[‡]The Biodesign Institute, and Department of Chemistry and Biochemistry, Arizona State University, 1001 McAllister Ave., Tempe, Arizona 85287, United States

ABSTRACT: The role of protein dynamics in guiding multistep electron transfer is explored in the photosynthetic reaction center of *Rhodobacter sphaeroides*. The energetics of the charge-separated intermediates, $P^+B_A^-$ and $P^+H_A^-$ (P is the initial electron donor bacteriochlorophyll pair and B_A and H_A are early bacteriochlorophyll and bacteriopheophytin acceptors, respectively), were systematically varied in a series of mutants. A fast phase of $P^+H_A^-$ recombination was resolved that is very sensitive to driving force. Either increasing or decreasing the relative free energy of $P^+H_A^-$ resulted in a more prominent fast recombination component, and thus a decreased yield forward electron transfer. The fast phase apparently represents $P^+H_A^-$ charge recombination via an activated state, probably $P^+B_A^-$ (B_A is situated between P and H_A). In wild type, this activated state is largely inaccessible, presumably due to dynamic stabilization of $P^+H_A^-$ within the first 100 ps. In mutants that change the energetics, the rate of decay via the activated state accelerates and that pathway becomes significant. The dynamic stabilization of the protein makes it possible to achieve a nearly optimum environment of H_A in wild type on two different time scales and for two rather different reactions. On the picosecond time scale, the energetics is nearly, though not perfectly, optimized for transfer between the excited state of P and H_A. After dynamic stabilization of the state $P^+H_A^-$, the environment is optimized to avoid rapid recombination of the charge-separated state and instead carry out forward electron transfer to the quinone with very high yield on the hundreds of picosecond time scale. Thus, by employing protein dynamics, the reaction center is able to optimize multiple reactions, on very different time scales involving the same reaction intermediate.

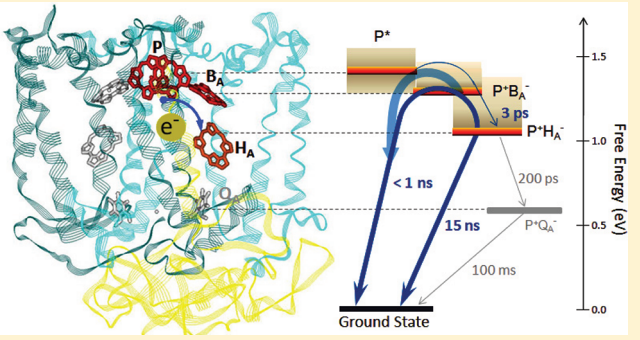

INTRODUCTION

While the role of protein structure in catalyzing enzymatic reactions is well-known, the mechanistic contribution of protein dynamics guiding the outcome of chemical reactions mediated by proteins is less clear. It is certainly the case that proteins stabilize specific transition states between reactant and product, but it is becoming increasingly clear that their function in chemical mechanism does not end there. In fact, at least in some cases, they appear to provide a dynamic potential landscape that uses conformational relaxation around the product state as one mode of avoiding unwanted back reactions and side reactions.

Here, this aspect of dynamic protein function is explored in the context of multistep electron transfer in the photosynthetic reaction center of *Rhodobacter sphaeroides*. The specificity and yield of each step are critical, as typically they involve reactive intermediates that have the potential to produce unwanted side products such as reactive oxygen species, or to simply return electrons to their source, wasting energy as heat. This kind of pathway presents a complex evolutionary optimization problem. In this case, the protein environment around a particular cofactor in the electron-transfer pathway must be simultaneously tuned to allow the cofactor to act both as a good acceptor in its neutral or oxidized state and as a good donor in its reduced or anion state. In addition, unwanted reactions, such as interaction with oxygen or return of the electron back to its source, must be minimized. The complexity is increased by the fact that the acceptor and donor reactions that a particular cofactor in the electron-transfer chain are involved in often occur on radically different time scales, necessitating a more or less independent tuning of these processes in different temporal regimes. In this respect, protein dynamics can play a critical role; what is stationary on one time scale may be flexible on another, creating a strongly time dependent chemical environment.

In wild-type purple bacterial reaction centers, the overall quantum yield of electron transfer from the initial donor to the final acceptor is almost 100% under low light conditions; this is a highly optimized system with essentially every photon absorbed, resulting in the formation of a charge-separated product (for review, see refs 1−4). Light absorption results in an excited

Received: November 17, 2011
Published: December 07, 2011

bacteriochlorophyll dimer, P*, which serves as the initial electron donor. Within a few picoseconds, an electron is transferred via a bacteriochlorophyll, B_A, to a bacteriopheophytin, H_A. This is followed by transfer of the electron to a quinone (Q_A) in approximately 200 ps.[1,5,6] Thus, the protein environment of the cofactor H_A must be optimized for its multiple roles: accepting an electron from P* in its neutral form on the picoseconds time scale and transferring an electron to Q_A on the 100 ps time scale in its anion form, all the while avoiding charge recombination (passing an electron back to P^+ re-forming the ground state).

The early electron-transfer reactions forming $P^+H_A^-$ are very robust and well studied; the overall rate and yield of this reaction depend only weakly on driving force and temperature and even in mutants where the forward rate is significantly compromised, the yield usually remains very high. The transfer from H_A to Q_A is less well studied, but it is known to be nearly temperature independent,[7] and substituting Q_A with a quinone that has a more negative midpoint potential is thought to slow the forward rate of electron transfer.[7−9] Replacing H_A with a bacteriochlorophyll molecule also substantially slows the forward rate.[10]

The yield of $P^+Q_A^-$ formation is determined by the competition between forward electron transfer and recombination. In the case of the picosecond electron-transfer reactions ($P^* \rightarrow P^+B_A^- \rightarrow P^+H_A^-$), the inherent lifetime of P* (the lifetime in the absence of electron transfer) is somewhere between 200 ps and a nanosecond (depending on how one blocks forward electron transfer[11]) in wild-type reaction centers. Thus, P* decay is about 100-fold slower than initial electron transfer and does not compete effectively with $P^+H_A^-$ formation. Similarly, forward electron transfer to the quinone from H_A^- is about 50-fold faster than recombination from the state $P^+H_A^-$,[6,12−15] again making this a high yield reaction in wild-type reaction centers.

As pointed out above, the competition between recombination and forward electron transfer determines reaction yield. Exploring the energetic landscape of charge recombination is a key component in understanding the how high yields are achieved. The only systematic study of the dependence of $P^+H_A^-$ recombination rate on the driving force used 5 ns wide excitation pulses to measure the recombination rates in wild type and a series of mutants in which the P/P^+ midpoint potential (and thus the reaction free energy for recombination to the ground state) had been changed over several hundred millielectronvolts (meV).[12] On the nanosecond time scale, nearly the same recombination rate was found for all samples (10−15 ns, depending on conditions), indicating that there was only a very weak dependence of the recombination kinetics on driving force. More recent studies have shown that under certain conditions (particularly reduced quinones) multiexponential charge recombination kinetics are observed.[16,17] This has been attributed to electrostatic interactions that decrease the energy between $P^+H_A^-$ and $P^+B_A^-$. As will be shown below, while the longer components of the $P^+H_A^-$ recombination are indeed essentially driving force independent, the early decay kinetics depend strongly on driving force. This finding is significant because it is recombination in the early time regime that competes with forward transfer forming $P^+Q_A^-$.

Here, a series of reaction center mutants are explored in which the relative free energy differences between $P^+B_A^-$, $P^+H_A^-$, and the ground state PBH are systematically varied. In contrast to previous studies, the $P^+H_A^-$ recombination rate in Q_A-depleted reaction centers is measured with picosecond resolution and particular attention is paid to recombination on the time scale of

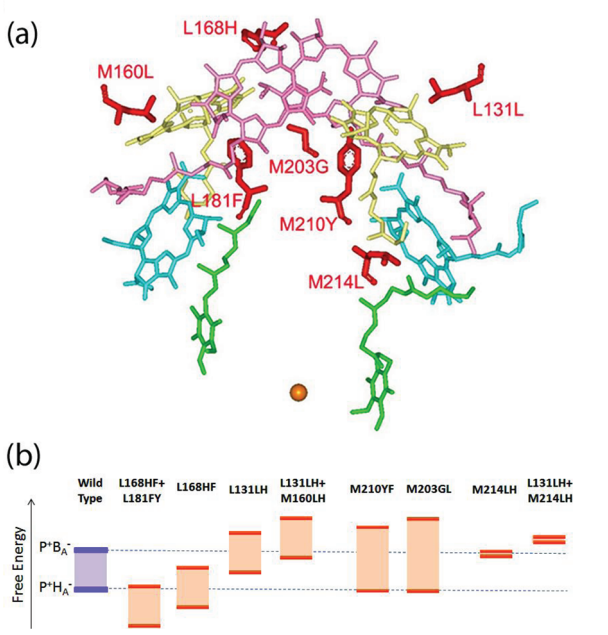

Figure 1. (a) Cofactor arrangement of wild-type reaction centers from *Rodobacter sphaeroides* (PDB code 2J8C) and the amino acid residues (shown in red) that were altered to vary the driving force for electron transfer. There were a total of eight different electron-transfer mutants used in this study, including single and double mutants of the residues shown. See text for details. (b) Schematic representation of the relative free energies of $P^+B_A^-$ and $P^+H_A^-$ from wild-type reaction centers and eight mutants. The free energy gap between $P^+B_A^-$ and $P^+H_A^-$ in each case is highlighted as a shaded region. The vertical axis (relative free energy) is not shown to scale.

normal electron transfer from H_A to Q_A. It is clear that, in wild type, the $P^+H_A^-$ state is sufficiently stabilized at early times to avoid wasteful recombination reactions. However, as the energetics of the system is changed, the product state stabilization becomes insufficient to avoid an apparent activated recombination via $P^+B_A^-$, presumably due to an acceleration of the inherent $P^+B_A^-$ recombination rate.

MATERIALS AND METHODS

The construction and expression of the mutants L168H → F (L168HF), L131L → H (L131LH), L131L → H + M160L → H (L131LH + M160LH), M210Y → F (M210YF), M203G → L (M203GL), and M214L → H (M214LH) were reported previously.[10,18−22] Two new double mutants L168H → F + L181F → Y (L168HF + L181FY) and L131L → H + M214L → H (L131LH + M214LH) were also constructed using methods described previously.[18−20] Figure 1a shows the cofactor arrangement and the amino acid residues that were altered in the mutants. Quinones were removed using published methods.[23] The purified reaction centers were suspended in 15 mM Tris-HCl (pH 8.0), 0.025% LDAO, and 1 mM EDTA. The samples were loaded into a 2 mm cuvette and stirred by a magnetic stir bar. The final optical density was about 1.0 at 800 nm.

Femtosecond transient absorption spectroscopy was performed as follows. A titanium sapphire oscillator (Tsunami, Spectra-Physics), was used to generate 100 fs, 800 nm laser pulses at a repetition rate of 82 MHz. These pulses were used to seed an optical amplifier system (Spitfire, Spectra-Physics), resulting in pulses of approximately 0.9 mJ at a repetition rate

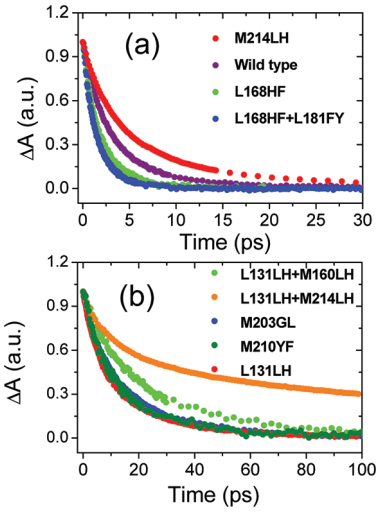

Figure 2. Initial electron-transfer kinetics measured for wild type and eight reaction center mutants determined by monitoring the decay of the stimulated emission signal from P* at 930 nm. Curves were normalized to their maxima at time zero.

of 1 kHz. Ten percent of the pulse energy was then used to generate a white light continuum for use as a probe beam by focusing it into a sapphire plate. The rest of the amplified 800 nm pulse was used to pump an optical parametric amplifier (OPA-800, Spectra-Physics), generating excitation pulses at a wavelength of 860 nm (second harmonic of idler beam). A measurement time window of 7 ns was achieved by double-passing the beam through the optical delay line. Transient absorption changes were measured using a monochromator (SP150, Action Res. Corp.) and a diode detector (Model 2032, New Focus Inc.). The decay of the excited state was monitored at 930 nm (stimulated emission of the state P*). $P^+H_A^-$ charge recombination was monitored at wavelengths between 830 and 845 nm, depending on the mutant (the probe wavelength was chosen to minimize interference by stimulated emission signals and the electrochromic shifts due to charge separation).

RESULTS

Initial Electron Transfer. Initial electron transfer and charge recombination kinetics were measured in wild type and eight different mutant reaction centers. The relative free energies of $P^+B_A^-$ and $P^+H_A^-$ are shown schematically in Figure 1b. Figure 2 compares the initial electron-transfer kinetics of wild type and eight reaction center mutants measured by monitoring the decay of the stimulated emission signal from P* at 930 nm. The overall electron-transfer rates in these mutants vary by more than an order of magnitude, from about 2 ps to tens of picoseconds. For the mutants L168HF and L168HF+L181FY that have a larger driving force for the initial electron transfer than wild type, the rate of the reaction actually increases. The remaining mutants show an overall slower stimulated emission decay. The electron-transfer dynamics and related energetics of these samples have been extensively studied previously.[10,24−29] Briefly, mutants L168HF, L168HF+L181FY, L131LH, and L131LH+M160LH are thought to primarily change the P/P^+ midpoint potential; mutants M210YF and M203GL appear to mainly vary the B_A/B_A^- midpoint potential; M214LH is the so-called β mutant in which the A-side bacteriopheophytin is replaced by bacteriochlorophyll, making the free energy of $P^+H_A^-$ very close to that of the $P^+B_A^-$. A newly designed mutant, L131LH+M214LH, is thought to affect the midpoint potentials of both P/P^+ and H_A/H_A^-, decreasing the free energy between $P^+H_A^-$ and P*, and results in a very slow electron-transfer rate, similar to that of L131LH alone.

Charge Recombination. Quinone-containing wild-type reaction centers were first measured as a control. The transient absorbance signal at 830 nm (blue side of the ground-state bleaching of P) is essentially time invariant; in this case, $P^+H_A^-$ converts to $P^+Q_A^-$ which is stable for milliseconds (Figure 3a). The 830 nm transient absorbance change in wild-type reaction centers without quinones decays on the nanosecond time scale due to charge recombination. This lifetime is consistent with previous reports.[2,12−14,30]

The mutants L168HF, L168HF+L181FY, L131LH, and L131LH+M160LH are thought to primarily shift the energy level of P without substantially changing the relative energetics between $P^+B_A^-$ and $P^+H_A^-$ (Figure 1b). Interestingly, the recombination dynamics during the first few nanoseconds depends strongly on the midpoint potential of P. This could not have been resolved in the previous charge recombination measurements as a function of P/P^+ potential due to the lower time resolution.[12] The initial recombination process is faster in all four of these mutants than in wild type (Figure 3a). This change is most pronounced for the L131LH+M160LH mutant, where more than 60% of the charge-separated state population decays to the ground state within 3 ns. Of particular note, L168HF and L168HF+L181FY both decrease the P/P^+ midpoint potential, while L131LH and L131LH+M160LH both increase the P/P^+ midpoint potential, yet all four mutations result in an increased amount of fast charge recombination. In principle, the fast recombination phase could originate from a static heterogeneous population of reaction centers that changes in different mutants. However, one might think that such static heterogeneity would also manifest itself in other measurements, such as excitation wavelength dependence of forward electron transfer, yet this is not observed.[31] Further, the systematic variation in the relative contribution of the two components between mutants suggests this kinetic feature is fundamental to the homogeneous function of reaction centers rather than an effect of multiple populations.

The mutants M210YF and M203GL are thought to primarily alter the B_A/B_A^- midpoint potential (presumably making reduction of B_A more difficult, Figure 1b). Thus, these mutations should increase the standard free energy difference between $P^+B_A^-$ and $P^+H_A^-$. The charge recombination reaction in these two mutants has kinetics very similar to wild type, dominated by a >10 ns decay, without a prominent fast process (Figure 3c).

In the mutant M214LH, the A-side bacteriopheophytin is replaced by bacteriochlorophyll, and the standard free energy between $P^+H_A^-$ (now $P^+\beta^-$) and $P^+B_A^-$ is thought to be nearly zero (Figure 1b).[10] The mutant L131LH+M214LH should change the midpoint potentials of both P/P^+ and H_A/H_A^-, again pushing $P^+H_A^-$ upward in energy and closer to $P^+B_A^-$. In both of these mutants, charge recombination is extremely fast (Figure 3d), with charge recombination times of 1 ns or less.

A summary of the results of fitting the charge recombination kinetics of wild type and the different reaction center mutants is given in Table 1.

DISCUSSION

Time-Dependent Solvation of the Charge-Separated State. Recently, several fast phases (700 ps to 3 ns) of $P^+H_A^-$

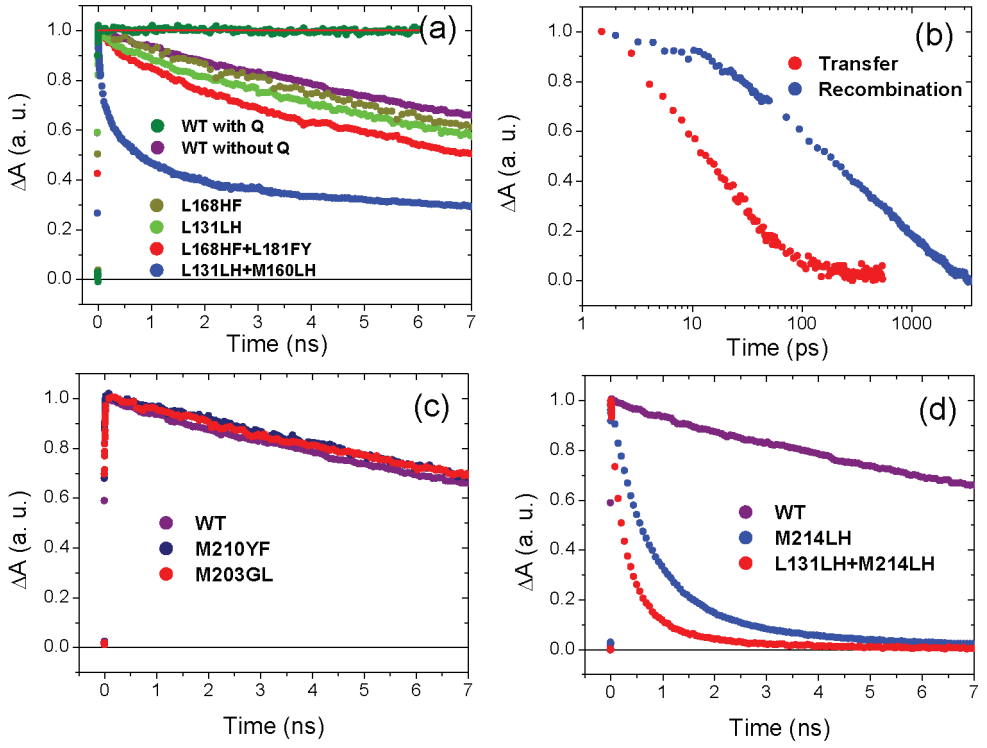

Figure 3. Decay kinetics of P^+ recorded at selected wavelengths between 830 and 845 nm (depending on the sample) for (a) quinone-removed reaction centers from wild type and four mutants that primarily shift the energy level of P as well as quinone-containing wild-type reaction centers; (c) quinone-removed wild-type reaction centers and two mutants that primarily alter the B_A/B_A^- midpoint potential; and (d) quinone-removed wild-type reaction centers and two mutants that primarily alter the H_A/H_A^- midpoint potential; (b) the absorbance changes at 930 nm (red) and 830 nm (blue) in quinone removed reaction centers from the L131LH+M160LH mutant were rescaled to their maxima and minima between 0 and 3 ns, and the two were compared on a log time scale.

Table 1. Charge Recombination Decay Lifetimes and Relative Amplitudes of the Fast and Slow Components Resulting from Multiple Exponential Fitting of Experimental Curve $f(t) = \Sigma_i A_i e^{-t/\tau_i}$, Where the Pre-exponential Factors A_i Are the Amplitudes of Each Component, and τ_i Are the Lifetimes[a]

fitting	wild type	L168HF+L181FY	L168HF	L131LH	L131LH+M160LH	M210YF	M203GL	M214LH	L131LH+M214LH
τ_0					0.06 ns			0.24 ns	0.12 ns
A_0 (%)					27%			13%	37%
τ_1	0.44 ns	0.9 ns	0.9 ns	0.6 ns	0.7 ns			0.8 ns	0.46 ns
A_1 (%)	3%	14%	2%	7%	32%			72%	55%
τ_2	17.0 ns	13.1 ns	14.7 ns	14.6 ns	20.1 ns	18.0 ns	18.5 ns	3.6 ns	2.4 ns
A_2 (%)	97%	86%	98%	93%	41%	100%	100%	15%	8%
τ_{ave}	16.5 ns	11.3 ns	14.4 ns	13.6 ns	8.5 ns	18.0 ns	18.5 ns	4.3 ns	0.5 ns

[a] The averaged lifetime, τ_{ave}, was calculated according to equation $\tau_{ave} = \Sigma_i A_i \tau_i / \Sigma_i A_i$.

recombination have been observed in wild-type reaction centers, particularly with Q_A in the reduced form, and have been attributed to activated re-formation of $P^+B_A^-$ at early times followed by relaxation of $P^+H_A^-$.[16,17] Here, much more pronounced multiexponential kinetics of charge recombination is observed in several mutants that change the energetics of charge-separated states (Figure 3 and Table 1). It has been known for many years that the free energy between P* and $P^+H_A^-$ is time dependent.[15,32,33] This has largely come from observing the fluorescence due to the quasiequilibrium formed between the charge-separated state and P* on the hundreds of picoseconds to nanoseconds time scale when further electron transfer to the quinone is blocked. Thus, a likely explanation of the kinetically heterogeneous $P^+H_A^-$ recombination, particularly obvious in some of the mutants studied here, is that this charge-separated state is initially in thermal equilibrium with $P^+B_A^-$ (and possibly P*, as has been previously suggested in refs 15 and 32−34) and relaxes relative to that state as a function of time. At very early times, P*, $P^+B_A^-$, and $P^+H_A^-$ are all likely within about 100 meV of each other. However, after several nanoseconds, the higher states become inaccessible and $P^+H_A^-$ decays directly to the ground state via a path that is not activated[15,34] (indeed, the temperature dependence of the nanosecond decay time of $P^+H_A^-$ is very weak[35]).

dx.doi.org/10.1021/jp211702b | J. Phys. Chem. B 2012, 116, 711–717

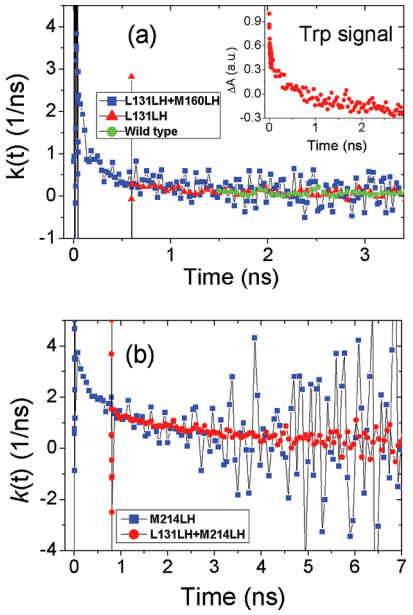

Figure 4. Comparing time-dependent charge recombination rates of various mutants. (a) Different P/P^+ midpoint potential mutants are compared to wild type with time scales shifted for comparison as described in the text. The inset shows the protein relaxation during the charge recombination as monitored by tryptophan absorbance changes at 280 nm. (b) The β mutant (M214LH) plus L131LH compared to the β mutant alone. Again, the time axis is shifted to show the similarity in kinetics as described in the text.

The relative free energy of $P^+H_A^-$ drops roughly 100 meV as the protein relaxes around the charge-separated state.[15,32,36] This protein solvation has been further confirmed by fast photoinduced potential measurements in reaction centers in the nanosecond time range.[37] It was found that under Q_A-reducing conditions, the photovoltage decayed significantly faster than the spectroscopically detected charge recombination of the radical pair $P^+H_A^-$, indicating the occurrence of considerable dielectric relaxations. When protein solvation takes place during charge recombination, in general, a time-dependent free energy difference $\Delta G(t)$ and recombination rate will result. The observation of highly nonexponential $P^+H_A^-$ recombination kinetics, especially for the mutants L131LH+M160LH, M214LH, and L131LH+M214LH, presumably reflects the effect of time-dependent solvation on the activation energy. Assuming that the mutations do not substantially affect the protein solvation processes (one reason for using multiple mutants with systematically varying energetics is to control any variation of this kind), one would expect that the time-dependent effective rate constant for charge recombination, $k(t)$, would change with time in a similar way from one mutant to another, even though the absolute value of $k(t)$ at any given time is dependent on the initial $P^+H_A^-$ or $P^+B_A^-$ energetics of the particular mutant. In particular, one would expect that $k(t)$ for reaction centers with an initial $\Delta G_1(0)$ would be the same as the $k(t + \Delta t)$ of reaction centers with an initial $\Delta G_2(0)$, where Δt is the time interval for the free energy drop represented by $[\Delta G_1(0) - \Delta G_2(0)]$ due to the protein solvation. The time-dependent rate, $k(t)$, can be calculated by $k(t) = -N^{-1}(t) \times dN(t)/dt$, where $N(t)$ is the population in the $P^+H_A^-$ or $P^+B_A^-$ state.

Figure 4 shows the comparison of $k(t)$ as a function of time for different reaction centers (Figure 4a, wild type, L131LH and L131LH+M160LH; Figure 4b, M214LH and L131LH+M214LH). The curves track each other quite closely once they are offset in time, consistent with the protein solvation model presented above. If one assumes that the initial ΔG change between mutants is approximately equal to the difference in the P/P^+ midpoint potentials ΔE_m of the mutants, then relative to L131LH+M160LH the ΔE_m are -50 and -130 meV for L131LH and wild type, respectively. Subsequently, the free energy of $P^+H_A^-$ appears to drop by 50 meV after 600 ps and by 136 meV after 1.5 ns. As described in detail previously,[29] one probe that has been used for monitoring the time scales of protein conformational dynamics is the time-dependent tryptophan absorbance changes at 280 nm. The tryptophan signal is shown in Figure 4a (inset), and includes picosecond to nanosecond protein relaxations over the 3 ns time window of the measurement. These relaxations are faster than the overall charge recombination reaction and consistent with the results obtained using fast photovoltage measurements.

Effect of Modulating B_A^- and H_A^- Energetics on Recombination. As seen in Figure 3d, and consistent with the earlier work cited above,[9] recombination in the β mutant exhibits a dominant, 800 ps (72%) process as well as two additional 240 ps (13%) and 3.6 ns (15%) components. In the L131LH+M214LH double mutant, the energies of $P^+B_A^-$ and $P^+\beta^-$ both increase, though the energy gap between them presumably remains the same as in the β mutant, M214LH. Recombination is faster in L131LH+M214LH, with time constants of 120 ps (37%), 460 ps (55%), and 2.4 ns (8%), implying that the recombination of $P^+B_A^-$, or $P^+\beta^-$ on the nanosecond time scale, is also dependent on the midpoint potential of P/P^+, as is $P^+H_A^-$. This could either reflect a change in the inherent lifetime of one of the charge-separated states in the double mutant or it could be due to the fact that P* is more energetically accessible facilitating that decay route. The fact that the most rapid recombination time constant is considerably faster than the inherent decay time of P* estimated from mutant studies (~200 ps)[38] supports the idea that the change in energetics accelerates the inherent recombination rate(s).

Further support for initial recombination of $P^+H_A^-$ via $P^+B_A^-$ comes from studying mutants that increase the free energy of $P^+B_A^-$ relative to $P^+H_A^-$. This should result in a decrease in the rate of early time $P^+H_A^-$ recombination. The mutations M210YF and M203GL are both thought to perturb B_A more than H_A. M210YF removes a tyrosine residue that is thought to interact with B_A, resulting in an increase in the free energy of $P^+B_A^-$. M203GL is thought to exclude a water molecule near B_A and also increase the $P^+B_A^-$ free energy. This should make $P^+B_A^-$ more difficult to access from $P^+H_A^-$, slowing recombination via that pathway. In Figure 3c, the recombination decay of wild-type reaction centers is compared to that of each of these mutants. While the difference is small, it is clear that these two mutants decay more slowly than wild type at early times. Kinetic analysis verifies that the 3% of the wild-type recombination that occurs with a 1 ns lifetime has disappeared in these mutants.

Midpoint Potential Dependence of Initial Charge-Separated State Recombination. The overall driving force dependence of $P^+H_A^-$ recombination can be determined by using mutants that change the P/P^+ midpoint potential without significantly altering the energy between $P^+B_A^-$ and $P^+H_A^-$.

This dependence has only been investigated in the past at low time resolution (5 ns).[6,12] In wild-type reaction centers, as shown here and previously,[16,17] only a small fraction of the $P^+H_A^-$ recombination occurs during the first nanosecond, and the resulting yield loss is low (~1%). The surprising result of this study, however, is that mutants that alter charge-separated state energetics and that have relatively small effects on the yield of initial electron transfer, or even increase the initial electron transfer rate (Figure 2), result in substantially greater recombination rate at early times of $P^+H_A^-$ (Figure 3), and therefore effectively compete with electron transfer to Q_A, significantly decreasing the yield of that reaction.

Four of the mutations studied either result in an increased (L131LH and L131LH+M160LH) or decreased (L168HF and L168HF+L181HY) P/P^+ midpoint potential. For L131LH and L131LH+M160LH, the P/P^+ midpoint potential increases by 80 and 130 meV relative to wild type, respectively, while the P/P^+ midpoint potential of L168HF decreases by 90 meV. The double mutant, L168HF+L181FY, is a combination of two mutants with decreased P/P^+ midpoint potentials; the actual midpoint has not been measured but the sum of the midpoints for the two mutations gives −150 meV. These mutants are thought to primarily affect the midpoint potential of P by forming hydrogen bonds to the macrocycles, rather than changing other energetic or structural aspects of the reaction center. Surprisingly, either increasing or decreasing the P/P^+ midpoint potential results in significantly faster rates of $P^+H_A^-$ recombination during the first nanosecond. In the mutant L131LH+M160LH, the effect of the mutation on the recombination rate of $P^+H_A^-$ is so great that one might think that the observed ground-state recovery of P reflects a yield loss during the initial electron-transfer reaction, rather than reflecting an increased $P^+H_A^-$ recombination rate. However, as shown in Figure 3b, stimulated emission from P* decays an order of magnitude faster than the rate of $P^+H_A^-$ recombination in Q_A-removed reaction centers and therefore initial electron transfer and charge recombination are not connected.

A Minimum in the Rate versus Free Energy Relationship for $P^+H_A^-$ Recombination. Generally, one would expect that, if anything, the rate of electron transfer would go through a maximum as a function of driving force, as described by Marcus' electron-transfer theory.[39] In contrast, what is observed here is a minimum in the rate versus driving force relationship for $P^+H_A^-$ recombination. The rate of recombination increases when the free energy of $P^+H_A^-$ relative to the ground state either increases or decreases from the wild type value. It certainly makes sense teleologically that wild-type reaction centers have been tuned to minimize the recombination reaction rate, in part by optimizing the energetics of $P^+H_A^-$.

A minimum in the rate versus free energy relationship for charge recombination suggests that there are at least two processes competing with one another that affect the rate. As described above, increasing both the free energy of $P^+H_A^-$ and $P^+B_A^-$ relative to wild type by increasing the P/P^+ midpoint potential as in the L131LH+M160LH mutant, likely results in a faster inherent recombination of $P^+B_A^-$ and thus an increase in the rate of activated $P^+H_A^-$ recombination at early times (Figure 3a). It is not as clear why the recombination rate would also increase when the free energy between the charge-separated states and the ground state was decreased relative to wild type. Formally, this could reflect the inherent rate versus driving force relationship for $P^+H_A^-$ recombination, but this effect is not obvious on longer time scales.

Optimizing the Yield of Charge Separation in Bacterial Reaction Centers. One of the puzzling aspects of initial electron transfer in reaction centers from *Rhodobacter sphaeroides* is the observation that the rate for this reaction can be increased by a couple of different individual mutations (L168HF and L181FY[40,41]). Certainly these mutations have arisen naturally many times during the evolution of the apparatus. However, optimizing the yield of photosynthetic charge separation involves more than just optimizing the yield of a single reaction. In this case, there are at least three reactions that involve the same cofactor engaged in the optimization: $P^* \rightarrow P^+H_A^-$, $P^+H_A^- \rightarrow P^+Q_A^-$, and $P^+H_A^-$ recombination to the ground state. Further, these reactions occur on different time scales. It appears that the protein environment of the photosynthetic reaction center addresses this complex time-dependent optimization process in part through a dynamic stabilization of $P^+H_A^-$. This allows the energetics of charge separation to be nearly (but not quite) optimal for initial electron transfer on the picosecond time scale, and then to adjust on the hundred picosecond time scale in such a way to maximize the yield of electron transfer to the quinone relative to recombination.

AUTHOR INFORMATION

Corresponding Authors

*E-mail: Haiyu_wang@jlu.edu.cn (H.W.); Nwoodbury@asu.edu (N.W.W.). Tel: 480-965-3294 (N.W.W.). Fax: 480-727-0396 (N.W.W.).

ACKNOWLEDGMENT

The authors acknowledge the financial support from NSF Grant MCB0642260 (N.W.W. and S.L.) and NSF of China Grant 20973081 (H.Y.W.). The authors also thank Dr. Jie Pan for assisting in the improvement of the optical setup and both Dr. Pan and Mr. Zhi Guo for useful discussions. Some of the mutants used in this work were originally prepared in the laboratory of Professors James Allen and JoAnn Williams.

REFERENCES

(1) Kirmaier, C.; Holten, D. *Photosynth. Res.* **1987**, *13*, 225–260.
(2) Woodbury, N.; Allen, J. In *Anoxygenic Photosynthetic Bacteria*; Blankenship, R. E., Madigan, M. T., Bawer, C. E., Eds.; Springer: Dordrecht, The Netherlands, 1995; pp 527−557.
(3) Wraight, C. A.; Gunner, M. R. In *The Purple Phototrophic Bacteria*; Hunter, C. N., Daldal, F., THurnauer, M. C., Beatty, J. T., Eds.; Springer: Dordrecht, The Netherlands, 2009; Vol. 28, pp 379−405.
(4) Parson, W. W.; Warchel, A. In *The Purple Phototrophic Bacteria*; Hunter, C. N., Daldal, F., Thurnauer, M. C., Beatty, J. T., Eds.; Springer: Dordrecht, The Netherlands, 2009; Vol. 28, pp 355−377.
(5) Zinth, W.; Kaiser, W. In *The Photosynthetic Reaction Center*; Deisenhofer, J., Norris, J. R., Eds.; Academic Press: San Diego, CA, 1993; Vol. II, pp 71−88.
(6) Woodbury, N. W.; Lin, S.; Lin, X. M.; Peloquin, J. M.; Taguchi, A. K. W.; Williams, J. C.; Allen, J. P. *Chem. Phys.* **1995**, *197*, 405–421.
(7) Gunner, M. R.; Dutton, P. L. *J. Am. Chem. Soc.* **1989**, *111*, 3400–3412.
(8) Gunner, M. R.; Robertson, D. E.; Dutton, P. L. *J. Phys. Chem.* **1986**, *90*, 3783–3795.
(9) Kirmaier, C.; Laporte, L.; Schenck, C. C.; Holten, D. *J. Phys. Chem.* **1995**, *99*, 8903–8909.
(10) Kirmaier, C.; Gaul, D.; Debey, R.; Holten, D.; Schenck, C. C. *Science* **1991**, *251*, 922–927.

(11) Chuang, J. I.; Boxer, S. G.; Holten, D.; Kirmaier, C. *Biochemistry* **2006**, *45*, 3845–3851.
(12) Tang, C. K.; Williams, J. A. C.; Taguchi, A. K. W.; Allen, J. P.; Woodbury, N. W. *Biochemistry* **1999**, *38*, 8794–8799.
(13) Shuvalov, V. A.; Parson, W. W. *Proc. Natl. Acad. Sci. U.S.A.—Biol Sci.* **1981**, *78*, 957–961.
(14) Schenck, C. C.; Blankenship, R. E.; Parson, W. W. *Biochim. Biophys. Acta* **1982**, *680*, 44–59.
(15) Ogrodnik, A.; Keupp, W.; Volk, M.; Aumeier, G.; Michelbeyerle, M. E. *J. Phys. Chem.* **1994**, *98*, 3432–3439.
(16) Gibasiewicz, K.; Pajzderska, M. *Photosynth. Res.* **2007**, *91*, 155–155.
(17) Gibasiewicz, K.; Pajzderska, M.; Ziolek, M.; Karolczak, J.; Dobek, A. *J. Phys. Chem. B* **2009**, *113*, 11023–11031.
(18) Lin, X.; Murchison, H. A.; Nagarajan, V.; Parson, W. W.; Allen, J. P.; Williams, J. C. *Proc. Natl. Acad. Sci. U.S.A.* **1994**, *91*, 10265–10269.
(19) Williams, J. C.; Haffa, A. L. M.; McCulley, J. L.; Woodbury, N. W.; Allen, J. P. *Biochemistry* **2001**, *40*, 15403–15407.
(20) Katilius, E.; Babendure, J. L.; Lin, S.; Woodbury, N. W. *Photosynth. Res.* **2004**, *81*, 165–180.
(21) Treynor, T. P.; Yoshina-Ishii, C.; Boxer, S. G. *J. Phys. Chem. B* **2004**, *108*, 13523–13535.
(22) Potter, J. A.; Fyfe, P. K.; Frolov, D.; Wakeham, M. C.; van Grondelle, R.; Robert, B.; Jones, M. R. *J. Biol. Chem.* **2005**, *280*, 27155–27164.
(23) Okamura, M. Y.; Isaacson, R. A.; Feher, G. *Proc. Natl. Acad. Sci. U.S.A.* **1975**, *72*, 3491–3495.
(24) Du, M.; Rosenthal, S. J.; Xie, X. L.; Dimagno, T. J.; Schmidt, M.; Hanson, D. K.; Schiffer, M.; Norris, J. R.; Fleming, G. R. *Proc. Natl. Acad. Sci. U.S.A.* **1992**, *89*, 8517–8521.
(25) Kalman, L.; Haffa, A. L. M.; Williams, J. C.; Woodbury, N. W.; Allen, J. P. *J. Porphyrins Phthalocyanines* **2007**, *11*, 205–211.
(26) Arlt, T.; Bibikova, M.; Penzkofer, H.; Oesterhelt, D.; Zinth, W. *J. Phys. Chem.* **1996**, *100*, 12060–12065.
(27) Spiedel, D.; Roszak, A. W.; McKendrick, K.; McAuley, K. E.; Fyfe, P. K.; Nabedryk, E.; Breton, J.; Robert, B.; Cogdell, R. J.; Isaacs, N. W.; Jones, M. R. *Biochim. Biophys. Acta—Bioenerg.* **2002**, *1554*, 75–93.
(28) Kirmaier, C.; He, C. Y.; Holten, D. *Biochemistry* **2001**, *40*, 12132–12139.
(29) Wang, H. Y.; Lin, S.; Allen, J. P.; Williams, J. C.; Blankert, S.; Laser, C.; Woodbury, N. W. *Science* **2007**, *316*, 747–750.
(30) Volk, M.; Ogrodnik, A.; Michel-Beyerle, M. E. In *Anoxygenic Photosynthetic Bacteria*; Blankenship, R. E., Madigan, M. T., Bauer, C. E., Eds. Kluwer: Dordrecht, The Netherlands, 2004; Vol. 2, pp 595—626.
(31) Wang, H. Y.; Lin, S.; Woodbury, N. W. *J. Phys. Chem. B* **2008**, *112*, 14296–14301.
(32) Peloquin, J. M.; Williams, J. C.; Lin, X. M.; Alden, R. G.; Taguchi, A. K. W.; Allen, J. P.; Woodbury, N. W. *Biochemistry* **1994**, *33*, 8089–8100.
(33) Pawlowicz, N. P.; Van Grondelle, R.; van Stokkum, I. H. M.; Breton, J.; Jones, M. R.; Groot, M. L. *Biophys. J.* **2008**, *95*, 1268–1284.
(34) Gibasiewicz, K.; Pajzderska, M. *J. Phys. Chem. B* **2008**, *112*, 1858–1865.
(35) Mcdowell, L. M.; Kirmaier, C.; Holten, D. *J. Phys. Chem.* **1991**, *95*, 3379–3383.
(36) Woodbury, N. W.; Parson, W. W. *Biochim. Biophys. Acta* **1986**, *850*, 197–210.
(37) Trissl, K.; B., M., L. *Biochemistry* **2001**, *40*, 5290–5298.
(38) Robles, S. J.; Breton, J.; Youvan, D. C. *Science* **1990**, *248*, 1402–1404.
(39) Marcus, R. A.; Sutin, N. *Biochim. Biophys. Acta* **1985**, *811*, 265–322.
(40) Huppmann, P.; Sporlein, S.; Bibikova, M.; Oesterhelt, D.; Wachtveitl, J.; Zinth, W. *J. Phys. Chem. A* **2003**, *107*, 8302–8309.
(41) Jia, Y. W.; Dimagno, T. J.; Chan, C. K.; Wang, Z. Y.; Du, M.; Hanson, D. K.; Schiffer, M.; Norris, J. R.; Fleming, G. R.; Popov, M. S. *J. Phys. Chem.* **1993**, *97*, 13180–13191.